Molecular Biology of the Cell
Vol. 20, 4458–4470, October 15, 2009

The Function of the Intermediate Compartment in Pre-Golgi Trafficking Involves its Stable Connection with the Centrosome

Michaël Marie, Hege A. Dale, Ragna Sannerud,* and Jaakko Saraste

Department of Biomedicine and Molecular Imaging Center, University of Bergen, N-5009 Bergen, Norway

Submitted December 22, 2008; Revised August 18, 2009; Accepted August 19, 2009
Monitoring Editor: Akihiko Nakano

Because the functional borders of the intermediate compartment (IC) are not well defined, the spatial map of the transport machineries operating between the endoplasmic reticulum (ER) and the Golgi apparatus remains incomplete. Our previous studies showed that the IC consists of interconnected vacuolar and tubular parts with specific roles in pre-Golgi trafficking. Here, using live cell imaging, we demonstrate that the tubules containing the GTPase Rab1A create a long-lived membrane compartment around the centrosome. Separation of this pericentrosomal domain of the IC from the Golgi ribbon, due to centrosome motility, revealed that it contains a distinct pool of COPI coats and acts as a temperature-sensitive way station in post-ER trafficking. However, unlike the Golgi, the pericentrosomal IC resists the disassembly of COPI coats by brefeldin A, maintaining its juxtaposition with the endocytic recycling compartment, and operation as the focal point of a dynamic tubular network that extends to the cell periphery. These results provide novel insight into the compartmental organization of the secretory pathway and Golgi biogenesis. Moreover, they reveal a direct functional connection between the IC and the endosomal system, which evidently contributes to unconventional transport of the cystic fibrosis transmembrane conductance regulator to the cell surface.

INTRODUCTION

The biosynthetic-secretory pathway sorts and delivers newly synthesized proteins and lipids, many with attached glycans, to the various endomembrane compartments of the cell and to its exterior (Palade, 1982). The dynamics and spatial organization of the secretory compartments—endoplasmic reticulum (ER), intermediate compartment (IC), and Golgi apparatus—depend on the microtubule (MT) and actin cytoskeleton and associated motor proteins (Thyberg and Moskalewski, 1999; Lippincott-Schwartz *et al.*, 2000; Allan *et al.*, 2002; Egea *et al.*, 2006). The prevailing paradigm of the secretory pathway in mammalian cells states that the Golgi apparatus, positioned around the MT-organizing center (MTOC)/centrosome (Rios and Bornens, 2003), receives nascent proteins from widely distributed ER exit sites (ERES) due to MT-dependent centralization of IC elements (Saraste and Svensson, 1991; Bannykh *et al.*, 1996; Presley *et al.*, 1997; Scales *et al.*, 1997; Hammond and Glick, 2000). After their post-translational modification and sorting in the Golgi, the proteins are distributed to the endolysosomal system, secretory granules, and the plasma membrane (PM; De Matteis and Luini, 2008). This spatial arrangement of the secretory process, consisting of centripetal and centrifugal transfer of biosynthetic products, is not essential for transport as such (Thyberg and Moskalewski, 1999; Hawes *et al.*, 2008). However, it can promote the coalignment of the secretory and endocytic routes, allowing their communication at multiple sites (Saraste and Kuismanen, 1992; Bonifacino and Rojas, 2006) and facilitate the processing and sorting of cargo along these pathways via the establishment of a lumenal pH gradient (Paroutis *et al.*, 2004). This topography may also be crucial for information transfer between endomembranes and the nucleus, and thereby for cell cycle progression (Sütterlin *et al.*, 2002), as suggested by the association of signaling molecules with the secretory compartments (Rios and Bornens, 2003; Sallese *et al.*, 2006).

According to the current map of the secretory pathway various proteins, such as lysosomal enzymes and PM proteins, follow the same route from ER to the *trans*-Golgi network (TGN), where they are sorted into different post-Golgi carriers (Griffiths and Simons, 1986; De Matteis and Luini, 2008). Accordingly, the TGN could equal to the central site where the direction of the secretory process is reversed. Brefeldin A (BFA), a drug that dissociates coat proteins (COPs) from IC/*cis*-Golgi (COPI) and TGN/endosomes (clathrin and adaptor proteins), revealed a functional division of the Golgi apparatus. During the ensuing MT-dependent Golgi disassembly *cis*-, medial-, and *trans*-Golgi compartments merge with the ER (Klausner *et al.*, 1992), whereas the TGN—as defined by TGN38 and the mannose-6-phosphate receptor that binds lysosomal enzymes—seems to fuse with an endosomal network that converges around the centrosome (Lippincott-Schwartz *et al.*, 1991; Wood *et al.*,

This article was published online ahead of print in *MBC in Press* (http://www.molbiolcell.org/cgi/doi/10.1091/mbc.E08–12–1229) on August 26, 2009.

* Present address: Laboratory for Membrane Trafficking, VIB, Department of Molecular and Developmental Genetics, and Center of Human Genetics, KULeuven, Campus Gasthuisberg, Herestraat 49, Box 602, 3000 Leuven, Belgium.

Address correspondence to: Jaakko E. Saraste (jaakko.saraste@biomed.uib.no).

Abbreviations used: BFA, brefeldin A; COP, coat protein; CFTR, cystic fibrosis transmembrane conductance regulator; CM, confocal microscopy; ERC, endocytic recycling compartment; GFP, green fluorescent protein; IC, intermediate compartment; MT, microtubule; pcIC, pericentrosomal domain of the IC; Tf, transferrin.

1991; Ladinsky and Howell, 1992; Reaves and Banting, 1992). Recently, specific knockdown of the BFA-sensitive factors that regulate membrane association of COPs at the two sides of the Golgi uncovered a similar borderline (Manolea *et al.*, 2008). Endosome–TGN communication has been implicated in retrograde transport of protein toxins and the cycling of transport machinery (e.g., the endopeptidase furin; Sandvig and van Deurs, 2002; Bonifacino and Rojas, 2006). Moreover, the endosomal system—in particular the endocytic recycling compartment (ERC), a pericentrosomal organelle with complex sorting functions (Maxfield and McGraw, 2004)—is emerging as an intermediate in biosynthetic transport to the PM (Hedman *et al.*, 1987; Futter *et al.*, 1995; Leitinger *et al.*, 1995; Orzech *et al.*, 2000; Harsay and Schekman, 2002; Yoo *et al.*, 2002; Ang *et al.*, 2004; Lock and Stow, 2005; Gravotta *et al.*, 2007).

Assuming continuous, vectorial flow of membranes toward the TGN, the IC elements operating at the ER–Golgi boundary could be seen as pleiomorphic transport carriers, which after their arrival in the Golgi region transform into or fuse with the *cis*-Golgi cisternae (Glick *et al.*, 1997; Bannykh *et al.*, 1998; Lippincott-Schwartz *et al.*, 2000). Alternatively, the transfer of cargo to the Golgi stacks could take place via IC tubules (Saraste and Kuismanen, 1984; Trucco *et al.*, 2004). The binding of COPI highlights the role of the IC in molecular sorting (Lowe and Kreis; 1998; Bannykh *et al.*, 1998); however, these coats are heterogeneous both in terms of their composition (Orci *et al.*, 1997; Wegmann *et al.*, 2004; Malsam *et al.*, 2005) and localization (Griffiths *et al.*, 1995; Martinez-Menarguez *et al.*, 1999; Moelleken *et al.*, 2007), and their roles in two-way traffic at the ER–Golgi boundary remain unclear (Pepperkok *et al.*, 1993; Peter *et al.*, 1993; Lippincott-Schwartz and Liu, 2006). Further, the IC consists of compositionally distinct vacuolar and tubular domains with specific roles in pre-Golgi trafficking (Sannerud *et al.*, 2006), correlating with the participation of COPI-dependent and -independent pathways in this process (Gaynor and Emr, 1997; Girod *et al.*, 1999; Morsomme and Riezman, 2002; Stephens *et al.*, 2002). The vacuoles contain Golgi-bound cargo and the cargo receptor p58/ERGIC-53 (Saraste and Svensson, 1991; Ying *et al.*, 2000; Horstmann *et al.*, 2002), which interacts with COPI coats (Kappeler *et al.*, 1997; Tisdale *et al.*, 1997). The tubules defined by the GTPase Rab1A (Palokangas *et al.*, 1998) extend from the vacuoles, join the peripheral and central IC elements into a dynamic membrane network and constitute a pathway that connects the IC with the cell periphery, bypassing the Golgi apparatus (Sannerud *et al.*, 2006). On the basis of the compositional and dynamic properties of the Rab1A-containing tubules, we proposed that they participate in Golgi-independent transport of cholesterol to the cell surface (Urbani and Simoni, 1990; Heino *et al.*, 2000; Sannerud *et al.*, 2006).

Here, live imaging of normal rat kidney (NRK) cells constitutively expressing fluorescent Rab1A enabled us to demonstrate that the tubular IC network, like the endosomal system, is stably anchored next to the centrosome, maintaining its dynamics after the Golgi apparatus has been disassembled by BFA. We provide evidence for communication between the pericentrosomal domain of the IC (pcIC) and the Rab11-positive ERC (i.e., the centrally located compartments of the two endomembrane networks), explaining how certain endocytosed molecules gain access to early secretory compartments and, conversely, how biosynthetic products, such as cholesterol and the cystic fibrosis transmembrane conductance regulator (CFTR) chloride channel, can bypass the Golgi apparatus on their way to the cell surface.

MATERIALS AND METHODS

Antibodies

The rabbit antisera against p58 and Rab1 were affinity-purified as described earlier (Saraste and Svensson, 1991; Sannerud *et al.*, 2006). Monoclonal anti-GM130, anti-p115, and anti-Rab11 were purchased from BD Transduction Laboratories (Lexington, KY), anti-HA from Nordic Biosite (Copenhagen, Denmark), and the polyclonal anti-green fluorescent protein (GFP), and anti-β-COP from Clontech (Palo Alto, CA) and Affinity BioReagents (Golden, CO), respectively. Monoclonal anti-β-tubulin was a kind gift from the late Thomas Kreis. Polyclonal antibodies were generously provided by the following: anti-γ-tubulin by Michel Bornens (Institut Curie, Paris, France), anti-mSec13 by Wanjin Hong (University of Singapore), anti-TGN38 by George Banting (University of Bristol, United Kingdom), anti-KDEL-receptor by Irina Majoul (Royal Holloway University of London, United Kingdom) and anti-mannosidase II by Kelley Moremen (University of Georgia). Polyclonal and monoclonal antibodies against the SFV spike glycoproteins were kindly provided by Esa Kuismanen (University of Helsinki, Finland) and Margaret Kielian (Albert Einstein College of Medicine, NY), respectively. Secondary antibodies, FITC- or Texas Red-coupled F(ab)-fragments of goat anti-rabbit and goat anti-mouse IgG were purchased from Jackson ImmunoResearch (West Grove, PA).

Generation of Stable NRK Cells Expressing GFP-Rab1A

The plasmid encoding pEGFP-Rab1A (Sannerud *et al.*, 2006) was used as a template for the following synthetic oligonucleotide primers: 5′-GGATACGCGTTCGCCACCATGGTGAG-3′ (MluI; forward primer) and 5′-GGGAATTCCATATGT-AGCAGCAACCTCCAC-3′ (NdeI) (Invitrogen, Carlsbad, CA) to generate MluI/GFP-Rab1A/NdeI fragments. The PCR products were cloned into the pCR 2.1-TOPO vector (Invitrogen), excised, gel purified, and subsequently inserted into the MluI/NdeI-linearized lentiviral vector pWPXL (Didier Trono laboratory, Ecole Polytechnique Fédérale de Lausanne, Lausanne, Switzerland) to generate pWPXL-GFP-Rab1A. The accuracy of the construct was verified by sequencing. To produce retroviral particles (Karolewski *et al.*, 2003), subconfluent HEK293T producer cells bound to poly-D-lysine–coated (BD Biosciences, San Jose, CA) dishes were transiently transfected using complete culture medium [DMEM containing fetal bovine serum (FBS; 10%), L-glutamine (2 mM), penicillin (50 U/ml), and streptomycin (50 μg/ml)] supplemented with SuperFect Transfection Reagent (QIAGEN, Chatsworth, CA), 3 μg of the vector genome plasmid, and 9 μg of ViraPower Lentiviral Packaging Mix (Invitrogen). At 48 h after transfection the virus-containing medium was harvested, centrifuged for 15 min at 3000 $\times$ *g*, filtered through a 45-μm filter (Schleicher & Schuell, Keene, NH), and stored in aliquots at −80°C. A stably transformed NRK cell line expressing GFP-Rab1A, produced during a 24-h infection with the virus supernatants in the presence of polybrene (1 μg/μl), was subjected to fluorescence-activated cell sorting (FACS) to give three subclones with various expression levels of GFP-Rab1A. The cells expressing the fusion protein at close to endogenous levels, as determined by Western blotting using antibodies against Rab1 and GFP (see Figure 1), were used for immunocytochemistry and live cell imaging.

Cell Culture, Synchronization, and Drug Treatments

The parental NRK, GFP-Rab1A–expressing NRK, HeLa, and BHK-21 cells were cultivated as described previously (Palokangas *et al.*, 1998; Sannerud *et al.*, 2006). The BHK cells stably expressing triple hemagglutinin (HA)-tagged CFTR (Sharma *et al.*, 2004) were passaged in complete DMEM supplemented with 1 μg/ml puromycin (Sigma). For synchronization, the GFP-Rab1A–expressing NRK cells, grown to 60–80% confluency, were presynchronized at G0 during a 48 h growth in medium containing low serum (0.5% FBS) or arrested at G1/S junction during a further 14-h incubation in complete DMEM containing 5 μg/ml aphidicolin (Sigma). Finally, the cells were examined by confocal microscopy (CM) or live cell imaging. BFA (Epicenter Technologies, Madison, WI) was used at 5 μg/ml and cycloheximide (Sigma) at 50 μg/ml. In washout experiments the BFA-treated cells were first extensively washed with prewarmed, drug-free medium, followed by incubation for different times at 37°C in the absence of BFA. To depolymerize MTs or actin filaments, the cells were treated for 30 min at 37°C with nocodazole (10 μg/ml; Sigma) or latrunculin B (1 μg/ml; Sigma), respectively. F-actin was detected with TRITC-labeled phalloidin (Sigma).

Virus Infection

Infection of the parental and GFP-Rab1A–expressing NRK cells with the temperature-sensitive mutant ts-1 of Semliki Forest virus (SFV ts-1) and their growth for 3.5 h at the restrictive temperature (39°C) were carried out as described earlier (Saraste and Kuismanen, 1984; Kuismanen and Saraste, 1989). After incubation at 39°C the cells were shifted for different time periods (10, 20, 30, 60, or 120 min) to the permissive temperature (28°C) or transferred for 1–2 h to low temperature (15 or 20°C) in the presence of cycloheximide. Alternatively, the cells were first shifted to 28°C for 5 min and then returned to 39°C for various periods of time (5, 10, 15, 30, or 60 min; Saraste and

Kuismanen, 1984). At harvest the cells were fixed for 30 min with 3% paraformaldehyde (PFA) in 0.1 M phosphate buffer, pH 7.5.

Uptake of Fluorescent Transferrin

To deplete endogenous transferrin the NRK cells expressing GFP-Rab1A were first incubated for 60 min in serum-free DMEM containing 0.2% BSA. Subsequently, another 60-min incubation in the same medium containing 20 μg/ml Alexa-Fluor 555–conjugated human transferrin (Molecular Probes, Eugene, OR) resulted in saturation of the compartments participating in the endocytic and recycling itineraries of the protein. Finally, the cells were washed with complete medium and fixed with 3% PFA, as above, or treated for 30 min with BFA before washing and fixation.

Immunofluorescence Staining and CM

Cells grown on glass coverslips were fixed for 30 min with 3% PFA as above or, alternatively (to preserve better the Rab1A-containing tubules in BFA-treated cells), in PFA-lysine-sodium periodate (2% PFA, 0.075 M lysine-HCl, and 0.01 M $NaIO_4$ in 0.375 M Na-phosphate buffer, pH 6.2). To localize β-tubulin, the cells were incubated for 30 min on ice and then fixed for 30 min at room temperature (RT) in 3% PFA in MT-stabilizing buffer (5 mM EGTA, 1 mM $MgCl_2$ in 70 mM PIPES buffer, pH 6.8). The immunofluorescence staining protocol has been described in detail elsewhere (Sannerud *et al.*, 2008). The samples were examined using Leica TCS SP2 AOBS (Leica Microsystems, Wetzlar, Germany) and Zeiss LSM 510 Meta (Carl Zeiss, Oberkochen, Germany) confocal microscopes using 63×/1.4 NA and 100×/1.4 NA HCX Plan-Apochromat (Leica), or 40×/1.3 NA Plan-Neofluor and 63×/1.4 NA Plan-Apochromat (Zeiss) oil-immersion objectives, ~1.2 airy unit pinhole aperture, and appropriate filter combinations. Images were acquired with 405 Diode, Argon ion/Argon Krypton (Leica) and Argon/Helium Neon (Zeiss) lasers. The acquired images were processed using the Photoshop CS2 image software (Adobe Systems, San Jose, CA). In the BFA washout experiments with CFTR-expressing BHK cells quantitation of the colocalization of HA-tagged CFTR and endogenous Rab1A in the pericentrosomal region and the expression of CFTR at cell surface involved a minimum of 200 randomly selected cells per time point. Similarly, to estimate the kinetics of Golgi reassembly, parallel samples were stained with anti-mannosidase II and the fraction of cells where the signal was confined to a single compact juxtanuclear structure was determined.

Live Cell Imaging

GFP-Rab1A–expressing NRK cells were grown on 35-mm glass-bottom culture dishes (MatTek, Ashland, MA; No. 1.5) in a constant 5% CO_2 environment at 37°C. Time-lapse CM was performed on a Zeiss LSM 510 Meta with a 40×/1.3 NA Plan-Neofluor oil-immersion objective, 3 airy unit pinhole aperture, and an Argon laser. Fast imaging was performed by using the UltraView RS Live Cell Imager (Perkin Elmer, Norwalk, CT). Samples were viewed with a 63×/1.4 NA Plan-Apochromat oil-immersion objective, and images were acquired at 512 × 512 resolution using a 488-nm excitation laser line. The CCD camera was operated at 1 × 1 binning. Time series were produced by collecting images at regular intervals, acquiring Z-stacks of part or the entire cell depth. The recorded images were converted to 8-bit TIFF files and further processed using the ImageJ software (National Institutes of Health; http://rsb.info.nih.gov/ij/). Still images were compiled using Adobe Photoshop CS2, and QuickTime movie sequences were assembled using Adobe Premiere Pro.

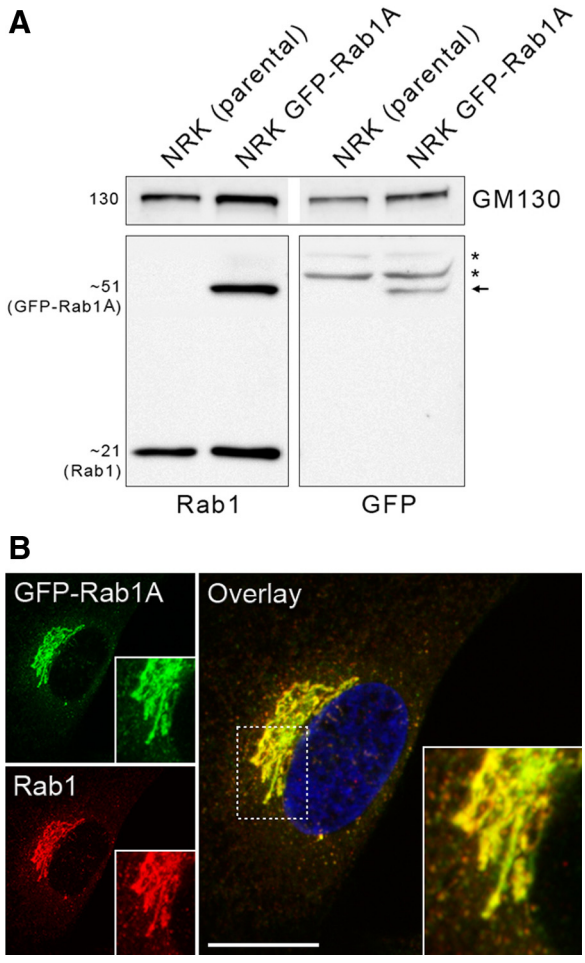

Figure 1. Characterization of the GFP-Rab1A–expressing cells. (A) Proteins in the postnuclear supernatants, prepared from parental NRK cells and the cells stably expressing low levels of GFP-Rab1A, were analyzed by SDS-PAGE and immunoblotting using antibodies against GM130 (loading control), Rab1 and GFP. Note the detection of the 51-kDa fusion protein (arrow) only in latter cells and the two additional bands (asterisks) in both lysates that react nonspecifically with anti-GFP. (B) The GFP-Rab1A–expressing cells were stained with anti-Rab1 and anti-rabbit IgG coupled to Texas Red. These maximum intensity projections show the normal appearance of the Golgi ribbon and the overlap between the green and red signals. Bar, 10 μm. See also Supplementary Movie 1.

RESULTS

Identification of the pcIC

The two Rab1 isoforms that regulate ER–Golgi trafficking, Rab1A and Rab1B, are both recruited to the peripheral IC at ERES, but show differential affinities to its tubular or vacuolar domains, respectively (Allan *et al.*, 2000; Sannerud *et al.*, 2006; Monetta *et al.*, 2007). To promote further studies of IC dynamics, we generated stable NRK cells expressing the previously described, GFP-coupled variant of Rab1A (Sannerud *et al.*, 2006). The expression level (Figure 1A) and distribution (Figure 1B) of GFP-Rab1A in these cells were similar to those of endogenous Rab1, and its expression did not affect the localization of the other IC and Golgi markers studied (see Figure 6). In addition, time-lapse CM showed that the cells remain motile and undergo apparently normal cell division (Supplementary Movie 1). Because previous immunolocalization studies of NRK cells demonstrated the typical association of Rab1 with pleiomorphic IC elements located close to the widespread ERES and the *cis*-face of the Golgi stacks (Saraste *et al.*, 1995; Palokangas *et al.*, 1998; Sannerud *et al.*, 2006; M. Marie and J. Saraste, unpublished data), it was of interest that time-lapse CM revealed the additional presence of GFP-Rab1A in large membrane clusters at the cell center, however, often at a considerable distance (up to 10 μm) from the Golgi ribbon (Supplementary Movie 1). To rule out that they result from mis-localization of the fusion protein, we reexamined the distribution of endogenous Rab1 in the parental NRK cells, as well as other cell types (HeLa and BHK cells) and could verify that they represent authentic structures (Figure 2A; see also Figure 9A). Notably, whereas about one-third of semiconfluent, actively growing cells express these clusters, they are much less frequent in stationary cultures (Figure 2, A and B).

Costaining of cells with antibodies against β- and γ-tubulin showed that the Rab1A-containing membrane clusters are located next to the centrosome (Figure 2, C and D). Although the p58-positive vacuolar IC elements (Saraste and

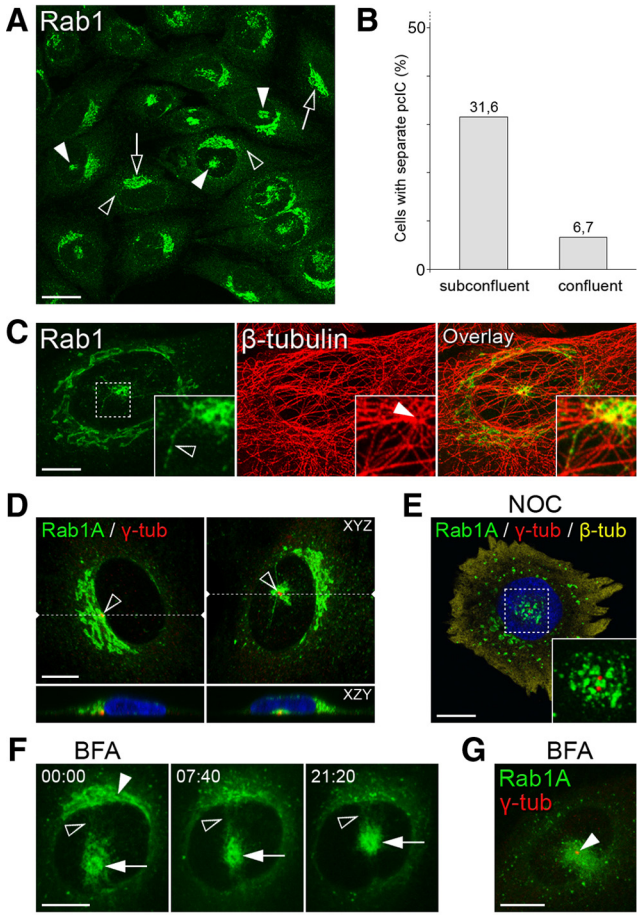

Figure 2. Identification of the pcIC. (A–C and D–G) The parental and stable GFP-Rab1A–expressing NRK cells, respectively. (A) Endogenous Rab1 localizes to peripheral IC (black arrowheads), *cis*-Golgi region (arrows), and centrally located membrane clusters (pcIC; white arrowheads). (B) Quantification showing that these novel clusters are readily detected in subconfluent (60–70%) cells, compared with confluent (~100%) cultures (n = 1100). (C) Double-staining for Rab1 and β-tubulin revealing their connection with the MTOC (inset, white arrowhead). The insets show the coalignment of pcIC tubules with MTs (inset, black arrowhead). (D) The location of the pcIC next to the Golgi ribbon (left) or under the nucleus (right) is linked to that of the centrosome marked by γ-tubulin (n = 115). The locations of the XZY projections (bottom panels) are indicated by the dashed lines in the top panels (XYZ). (E) The central location of the pcIC is maintained in NOC-treated cells (n = 20), as shown by triple imaging of GFP-Rab1A, the duplicated centrosome (γ-tubulin), and β-tubulin (cytosolic). (F) Dynamics of GFP-Rab1A–positive membranes in BFA-treated cells was recorded by spinning disk CM (Supplementary Movie 2), starting at the time of drug addition (time = min:sec). Note the dispersal of the juxtanuclear "*cis*-Golgi reticulum" (white arrowhead), the persistence of the central pcIC (white arrows) and ongoing communication between the two locations (black arrowheads). (G) Colocalization of the pcIC and the centrosome (γ-tubulin) in cells treated for 30 min with BFA. Bars, (A) 20 μm; (C–G) 10 μm.

Svensson, 1991; Ying *et al.*, 2000; Sannerud *et al.*, 2006) are also found in this region, they display a more dispersed pattern (see Figure 6B). Below, we use the term pcIC (pericentrosomal domain of the IC) when referring to these structures. Electron microscopy further showed that the pericentrosomal, Rab1A-positive tubules and vesicles below the nucleus (see Figure 2D) constitute part of a complex membrane system, which does not display Golgi-type cisternal

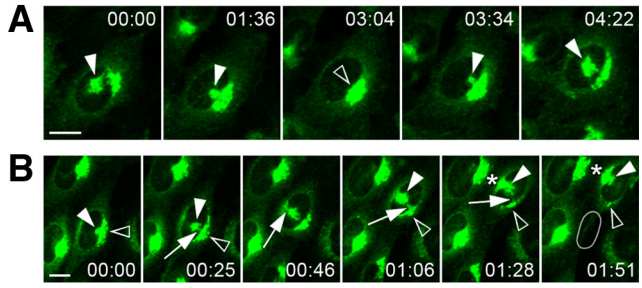

Figure 3. Time-lapse CM shows the mobility of the pcIC. (A and B) Selected images from Supplementary Movies 3 and 5, respectively (time = hr:min). (A) Reversible detachment of the pcIC from the Golgi ribbon, which is coupled with its expansion (n = 7). (B) The mobile pcIC acts as an intermediate during Golgi repositioning in a migrating cell (n = 8). The original position of the nucleus is indicated in the last panel. Bars, 10 μm.

organization (data not shown; however, see Tooze and Hollinshead, 1992). The tubules also extend toward the cell periphery, coaligning with centrosomal MTs (Figure 2C; see also Figure 4H). In contrast to its well-known effects on the Golgi (Thyberg and Moskalewski, 1999), depolymerization of MTs by nocodazole leads to fragmentation of the Rab1-positive pcIC, but did not affect its central positioning (Figure 2E), indicating that the association of the pcIC membranes with the centrosome does not solely depend on their centralization along MTs. Similar results were obtained using latrunculin B, which breaks down actin filaments (data not shown).

To further study the relationship of the pcIC with the Golgi apparatus, we use BFA, which removes membrane-bound COP coats and results in Golgi disassembly (Klausner *et al.*, 1992). Spinning disk CM of GFP-Rab1A showed that the dispersal of the IC membranes residing at the *cis*-face of the Golgi apparatus—like that of Golgi stacks (Sciaky *et al.*, 1997)—is complete by ~8 min of BFA addition (Figure 2F; Supplementary Movie 2), coinciding with an increased GFP-Rab1A signal in IC elements at nearby ERES (Supplementary Movie 2; see also Figure 7B). Interestingly, in contrast to the Golgi ribbon, the Rab1-positive pcIC resists the disassembly of COPI coats and maintains its pericentrosomal positioning (Figure 2, F and G; Supplementary Movie 2), revealing the stability and functional specialty of this novel IC domain. Although the pcIC also retains its tubular organization in the drug-treated cells, as demonstrated by live cell imaging (Figure 2F; see also Figure 7A; Supplementary Movie 2), the tubules are especially sensitive to fixation, resulting in diffuse appearance of this compartment (Figure 2G).

Mobility and Plasticity of the pcIC

The positioning of the pcIC strictly correlates with that of the centrosome. Accordingly, it is either masked by the Golgi ribbon or is present as a distinct structure because of the relocation of the centrosome below the nucleus (Figures 2D and 3). Examination of pcIC dynamics by time-lapse CM revealed that its separation from the Golgi is coupled to cell migration or division (Supplementary Movie 1; i.e., events that involve centrosome motility; Rios and Bornens, 2003). However, separation also takes place in interphase cells arrested at the G0 and S phases of the cell cycle (data not shown), suggesting that it is coupled to other processes, as well. Indeed, the pcIC reversibly changes its location in stationary cells, remaining isolated for several hours (Figure

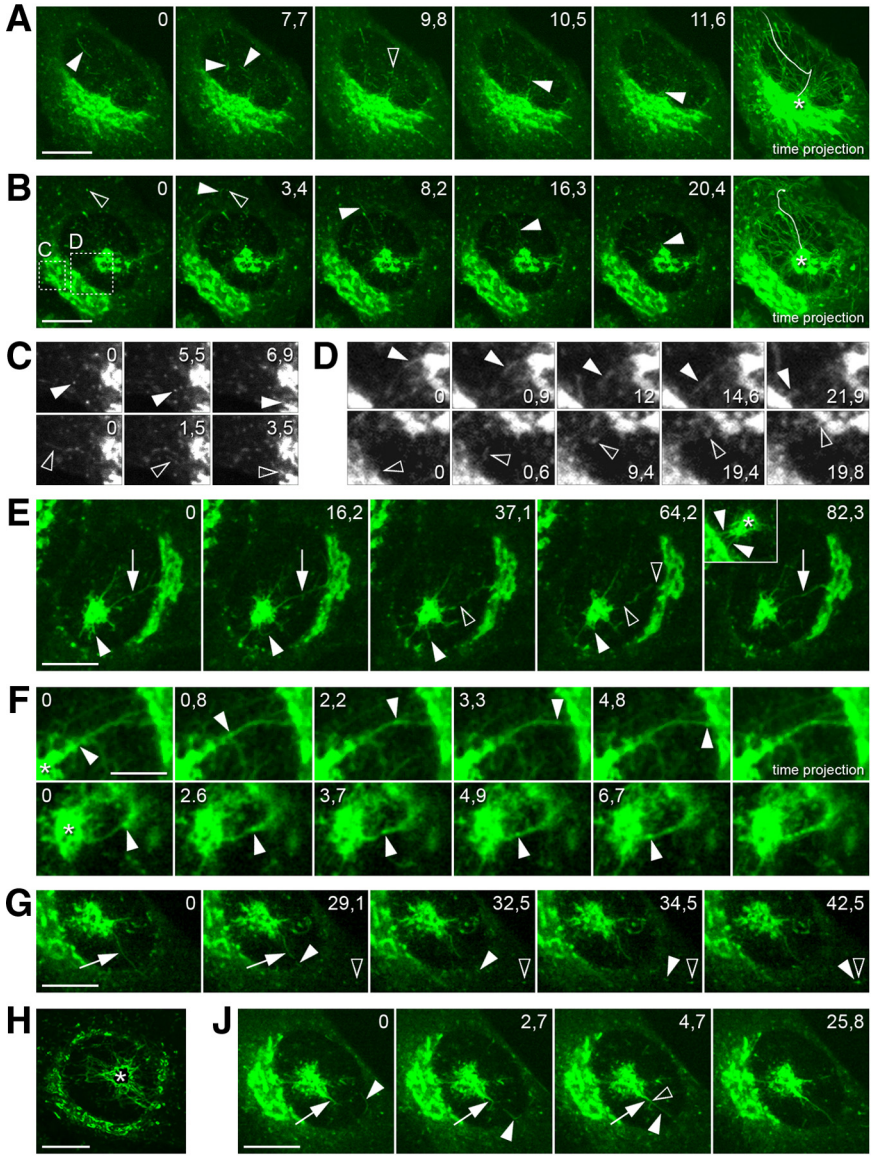

Figure 4. Role of the pcIC in pre-Golgi membrane dynamics. (A–D) The movements of pleiomorphic IC elements were recorded by spinning disk CM. (A and B) Selected images from Supplementary Movies 6 and 7 (time = sec) of GFP-Rab1A–expressing cells, in which the pcIC is either masked or unmasked by the Golgi, respectively. The last panels show time projections, highlighting the paths of tubular elements that move from the peripheral ERES toward the pcIC (asterisks). The tracks of individual tubules are indicated by arrowheads (images) and plain lines (time projections). In A the tubule changes direction as it shifts from one MT track to another (black arrowhead). In B the tubule originating at a peripheral ERES (black arrowhead) moves directly toward the pcIC. (C and D) The regions indicated in B at higher magnification. In C "vesicular" (top row, white arrowheads) and tubular (bottom row, black arrowheads) elements move directly toward and join the Golgi, whereas in D two-way communication between the pcIC and the Golgi ribbon takes place via similar structures. (E) The formation of transient tubular continuities (arrows) between the pcIC and the Golgi ribbon. These images (see Supplementary Movie 8) show the breakage (black arrowheads) and rapid reformation (last frame, arrow) of such connections. The white arrowheads denote a tubule protruding from the pcIC that suddenly retracts. The inset (asterisk = pcIC) corresponds to Supplementary Movie 9, showing the formation of numerous tubular pcIC-Golgi continuities (white arrowheads). (F) Selected images from two movies (the top panels are from Supplementary Movie 4), documenting bidirectional movement of boluses (white arrowheads) along the pcIC-Golgi connections. (G) A short tubule (white arrowheads) pinches off from a pcIC tubule (arrows) and moves toward a peripheral site (ERES; black arrowhead). (H) Time projection of successive images from a movie (not shown) on an expanding, polygonal pcIC network. (J) A preexisting pcIC tubule (white arrows) grows in length due to fusion (black arrowhead) of an incoming tubule (white arrowheads). Bars, 10 μm, except in F, 5 μm.

3A; Supplementary Movie 3). Strikingly, the integrity of the Golgi apparatus remains unaffected by the separation, possibly because of its ongoing communication with the pcIC (see below) and/or ability to nucleate its own MTs (Chabin-Brion *et al.*, 2001). The detachment of the pcIC is regularly accompanied by its expansion (i.e., the compartment grows as it moves away from the Golgi ribbon) and, conversely, turns more compact before merging with it again (Figure 3A; Supplementary Movie 3). Expansion involves the formation of a polygonal tubular network (Palokangas *et al.*, 1998), which undergoes continuous remodeling due to extension, retraction, branching and shedding of tubules (see Figure 4, E and H; Supplementary Movie 4). More stationary pcIC tubules can grow at their tips via the attachment of incoming, mobile IC elements, or the latter are adsorbed into the pericentrosomal network (Figure 4J).

In motile cells the separation of the pcIC from the Golgi ribbon is frequently followed by the repositioning of the latter to the juxtanuclear pole facing the leading edge (Figure 3B; Supplementary Movie 1). Time-lapse CM revealed that the pcIC acts as an intermediate during the Golgi transfer, in line with the proposal that this process involves dis- and reassembly rather than mechanical displacement of the organelle (Bisel *et al.*, 2008). Apparently, membranes are first conveyed from the original Golgi to the central, expanding pcIC, which eventually joins the nascent Golgi on the other side of the nucleus (Figure 3B; Supplementary Movie 5). Based on spinning disk CM, such bulk membrane transfer may occur via tubular connections between the pcIC and the Golgi stacks (Supplementary Movie 4).

Participation of the pcIC in ER–Golgi Trafficking

To study the role of the pcIC in post-ER trafficking, we first used GFP-Rab1A as a marker in live cell imaging. Spinning disk CM showed that in cells where the pcIC is masked by the Golgi, pleiomorphic transport intermediates containing GFP-Rab1A move from ERES toward the Golgi ribbon along curvilinear paths, following MT tracks (Figure 4A; Sannerud *et al.*, 2006). Most of the predominantly tubular intermediates (Simpson *et al.*, 2006) move toward a specific site in the Golgi ribbon (Figure 4A, time projection; Supplementary Movie 6), evidently corresponding to the position of the

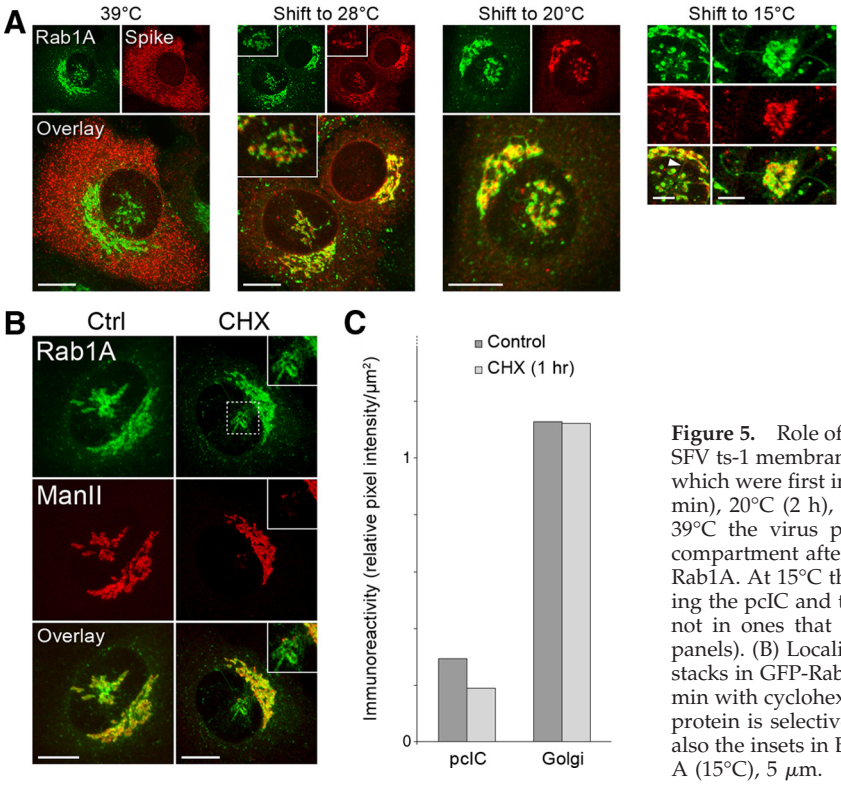

Figure 5. Role of the pcIC in ER–Golgi trafficking. (A) Localization of SFV ts-1 membrane proteins in infected GFP-Rab1A–expressing cells, which were first incubated at 39°C (3.5 h) and then shifted to 28°C (30 min), 20°C (2 h), or 15°C (2 h) in the presence of cycloheximide. At 39°C the virus proteins are absent from the pcIC, but enter this compartment after the temperature shifts, partially overlapping with Rab1A. At 15°C the proteins are also detected in the tubules connecting the pcIC and the Golgi ribbon (left panels, white arrowhead), but not in ones that extend from the pcIC to the cell periphery (right panels). (B) Localization of mannosidase II to the pcIC and the Golgi stacks in GFP-Rab1A–expressing control cells and cells treated for 60 min with cycloheximide. (C) Quantification (n = 35) showing that the protein is selectively, but only partially, depleted from the pcIC (see also the insets in B) in response to cycloheximide. Bars, 10 μm, except A (15°C), 5 μm.

centrosome (Figure 1D). In addition, some join the Golgi at other locations; however, their target sites could not be identified. Notably, in cells expressing a separate pcIC, the IC elements predominantly move toward this centrally located network (Figure 4B, time projection; Supplementary Movie 7). Although part of the elements still target the Golgi (Figure 4C), they do not show the same directionality as seen in cells where the pcIC is masked by this organelle.

To verify that the pcIC operates in the transport of secretory cargo, the GFP-Rab1A–expressing cells were infected with a temperature-sensitive mutant of Semliki Forest virus (SFV ts-1). In cells kept at 39°C the ts-1 membrane proteins are arrested in the ER, whereas shift to 28°C triggers their synchronized transfer via the Golgi to the PM (Saraste and Kuismanen, 1984). Examination of cells kept at 39°C showed the absence of the virus glycoproteins from the pcIC region (Figure 5A), showing that it is devoid of rough ER, as well as ERES (Supplementary Figure S1A). By contrast, in cells shifted to 28°C in the presence of cycloheximide the virus proteins appeared in the pcIC (Figure 5A). Examination of cells shifted for different times (10–120 min) to 28°C indicated that the proteins enter the pcIC and the Golgi region simultaneously. Similar results were obtained even when the cargo load in post-ER compartments was restricted by exposing the cells only for 5 min to 28°C, followed by shift back to 39°C. After longer times at 28°C the pcIC pool of the proteins was reduced (data not shown). Interestingly, shift of cells to 15 or 20°C, to establish transport blocks at the IC or *trans*-Golgi, respectively (Saraste and Kuismanen, 1984), lead in both cases to pericentrosomal accumulation of the SFV proteins (Figure 5A). Notably, the bulk of the proteins does not reach the TGN during the 20°C block, as expected (Griffiths and Simons, 1986), but a considerable fraction remains arrested in the pcIC. Experiments with the vesicular stomatitis virus G protein showed that its ER-to-Golgi transfer also involves the pcIC (data not shown).

At 15°C the SFV glycoproteins were also detected in GFP-Rab1A–positive tubules, which connect the pcIC with the Golgi stacks (Figure 5A), most likely mediating their transfer between these compartments (Saraste and Kuismanen, 1984). Spinning disk CM further showed that these tubules establish transient continuities at the pcIC-Golgi boundary (Figure 4E and inset; see Supplementary Movies 8 and 9), creating tracks for bidirectional movement of bolus structures (Figure 4F; Supplementary Movie 4). Two-way traffic between the pcIC and Golgi also occurs in a discontinuous manner via tubular and vesicular intermediates (Figure 4D).

Localization of Golgi mannosidase II (Man II) to the pcIC (Figure 5B) suggested that this compartment also participates in the trafficking of endogenous cellular proteins. However, the pcIC pool of Man II, which is enriched in *cis*- and medial Golgi cisternae and has a half-life of ~20 h (Moremen and Touster, 1985), is relatively small (Figure 5C) and is highly variable—in some cells negligible (data not shown), most likely reflecting the different functional states of the cell that involve centrosome motility. To study the nature of this pool, cells were treated with cycloheximide to arrest protein synthesis, and the Man II signals of the separate pcICs and the Golgi stacks were determined. Compared with control cells, the pcIC pool was reduced by one-third after the drug treatment, whereas the Golgi pool remained unaffected (Figure 5C). Thus, ER-derived Man II is at least partly transported to the Golgi via the pcIC, as also shown by BFA washout experiments (see Supplementary Figure S2), whereafter the protein can cycle between the pcIC and the Golgi stacks.

The pcIC Contains Transport Machinery

The separation of the pcIC from the Golgi (Figure 2B) made it possible to study in more detail the localization of cargo and machinery proteins. Membrane-bound COPI coats

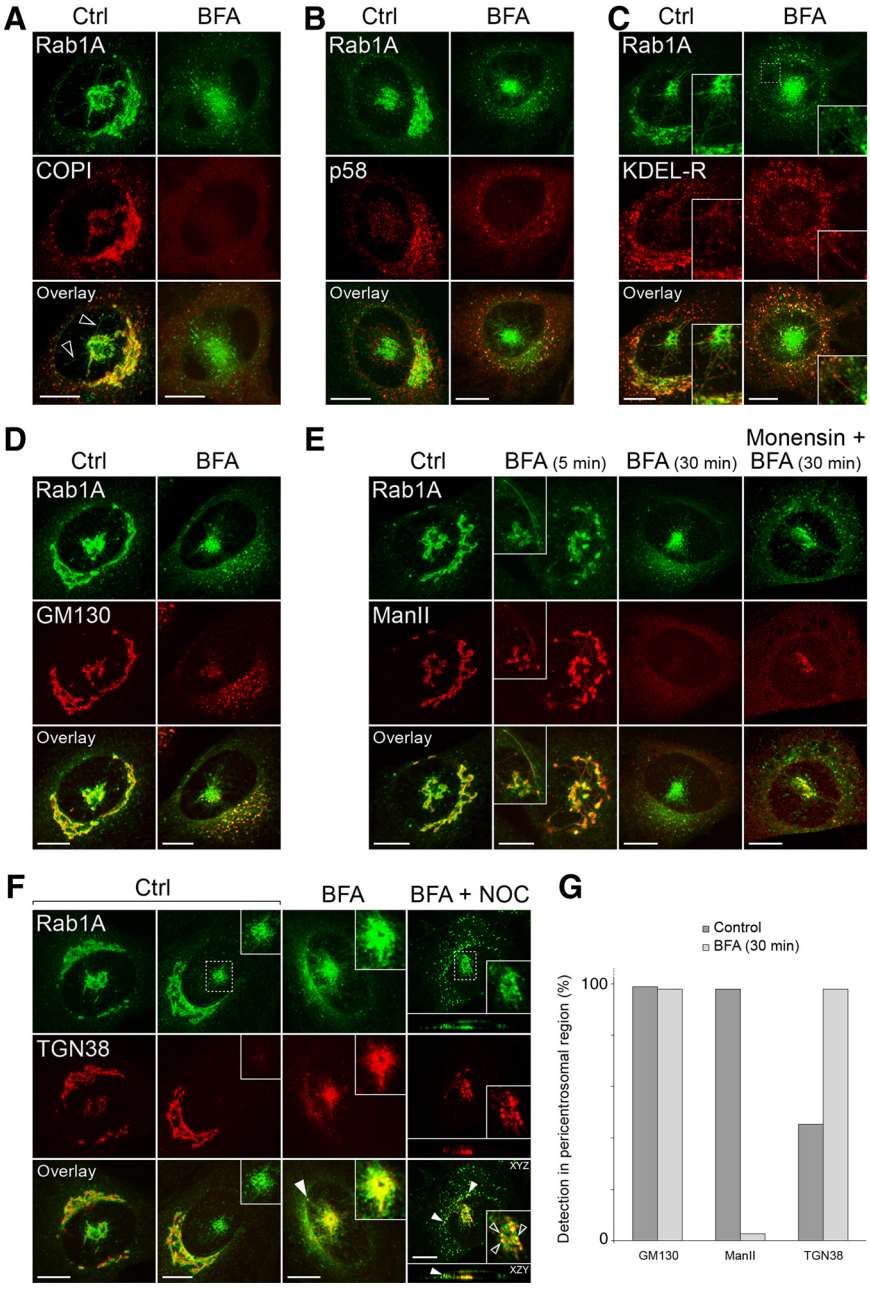

Figure 6. The mobility of the pcIC facilitates protein localization. Control NRK cells expressing GFP-Rab1A, and cells treated for different times (5 or 30 min) with BFA, were stained with antibodies against β-COP (A), p58 (B), KDEL-R (C), GM130 (D), mannosidase II (E), and TGN38 (F). In addition, the right panels in E and F show the localizations of mannosidase II on TGN38 in cells treated for 30 min with a combination of BFA + monensin or BFA + nocodazole, respectively. (G) Determination of the percentage of cells showing pericentrosomal labeling for GM130, mannosidase II and TGN38 (n = 250). Note that the cells were simply scored as positive or negative, irrespective of the intensity of the fluorescent signals, which were highly variable. Bars, 10 μm.

could be resolved into three spatially distinct, BFA-sensitive pools associating with peripheral IC, pcIC, or Golgi membranes, respectively (Figure 6A). COPI overlaps with GFP-Rab1A in the more compact regions of the pcIC, but is not readily detected along the tubules extending from it (Figure 6A). Strikingly, the KDEL-receptor (KDEL-R) and p58—transport receptors, which cycle at the ER–Golgi boundary in a COPI-dependent manner (Girod *et al.*, 1999), displayed differential distributions in the pericentrosomal region. Unlike p58, which is enriched in punctate IC elements in this area (Figure 6B), the KDEL-R colocalizes with Rab1A in the tubular network (Figure 6C). The latter maintains its localization in BFA-treated cells (Figure 6C, insets), whereas p58 relocates to peripheral IC elements and the ER (Figure 6B; Saraste and Svensson, 1991).

Interestingly, the pcIC contains distinct pools of the golgins GM130 (Figure 6, D and G) and p115 (Supplementary Figure S1B), i.e. Rab1 effectors that are implicated in homotypic fusion of IC elements and Golgi biogenesis (Sztul and Lupashin, 2006). GM130 maintains its association with the pcIC in BFA-treated cells (Figure 6, D and G)—in accordance with results showing that it contributes to centrosomal organization (Kodani and Sütterlin, 2008), and membrane binding of p115 also remains unaffected (Sztul and Lupashin, 2006). Like Man II, TGN38, which cycles between the TGN, the endosomal system and the PM (Bonifacino and Rojas, 2006), displays a highly variable signal in the pcIC area of control cells, whereas BFA leads to its accumulation at a pericentrosomal site (Lippincott-Schwartz *et al.*, 1991; Ladinsky and Howell, 1992; Reaves and Banting, 1992), most likely the ERC (Figure 6, F and G; see also Figure 8A). However, additional nocodazole treatment revealed that TGN38 partly overlaps with GFP-Rab1A (Figure 6F), suggesting that it can also move to the pcIC.

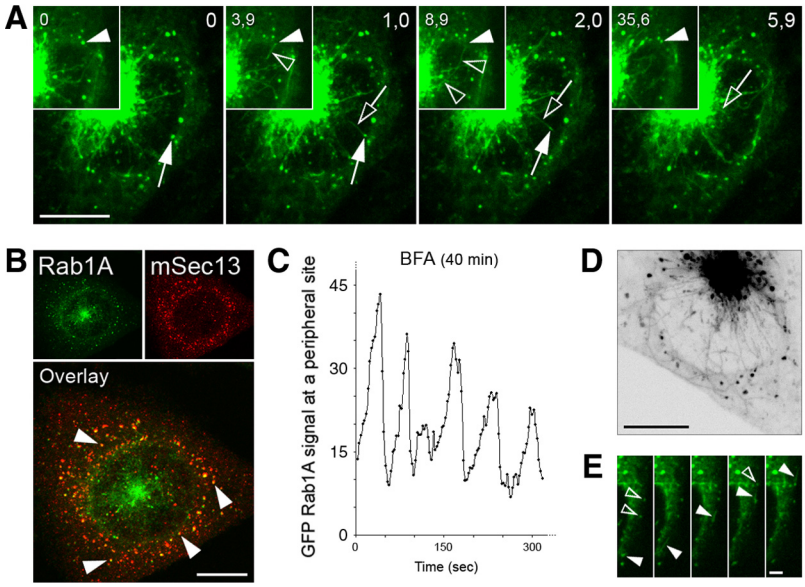

Figure 7. The IC maintains its dynamics after Golgi disassembly. (A) Live cell imaging by spinning disk CM shows the movements of GFP-Rab1A–positive IC elements in cells treated for 40 min with BFA. Selected images from Supplementary Movie 10 are shown (time = sec). Narrow tubules (black arrows) that extend from peripheral sites (ERES; white arrows) move toward and join the pcIC. The inset shows a stationary IC element (white arrowheads) transforming into a mobile tubule (black arrowheads) that merges with the pcIC. Note reappearance of the GFP signal at the original location. (B) Peripheral IC elements (white arrowheads) in BFA-treated cells (30 min) localize close to the ERES marked by the COPII coat subunit mSec13. (C) Recruitment of GFP-Rab1A to peripheral IC elements is not affected by BFA (40 min), as shown by the oscillation of their GFP signals (n = 17). (D and E) In BFA-treated cells (45 min) a tubular network extends from the pcIC toward the cell periphery (Supplementary Movie 11). The tubules interconnect "globular" IC elements (E) and are also found close to the PM. See also Supplementary Movie 12. (E) A tubule (white arrowheads) passes through two neighboring globular IC elements (black arrowheads). Bars, (A, B and D) 10 μm; (E) 2 μm.

The pcIC Is a Monensin-sensitive Compartment

In contrast to control cells (Figures 5B and 6E), shortly after addition of BFA Man II was detected in GFP-Rab1A–positive tubules connecting Golgi elements with the pcIC (Figure 6E, BFA 5 min) or extending from the latter toward the cell periphery (Figure 6E, inset), indicating that the pcIC acts as a way station during the transfer of Man II to the ER (Figure 6E, BFA 30 min). The separation of the pcIC from the Golgi allowed us to map the site where neutralization of acidic compartments affects the BFA-induced back-flow of Golgi components (Palokangas *et al.*, 1998; Barzilay *et al.*, 2005). Notably, Man II was partly arrested in the pcIC in the additional presence of monensin (Figure 6E), providing evidence that the pcIC maintains a low lumenal pH, which could facilitate its function in post-ER sorting events (see Figure 10).

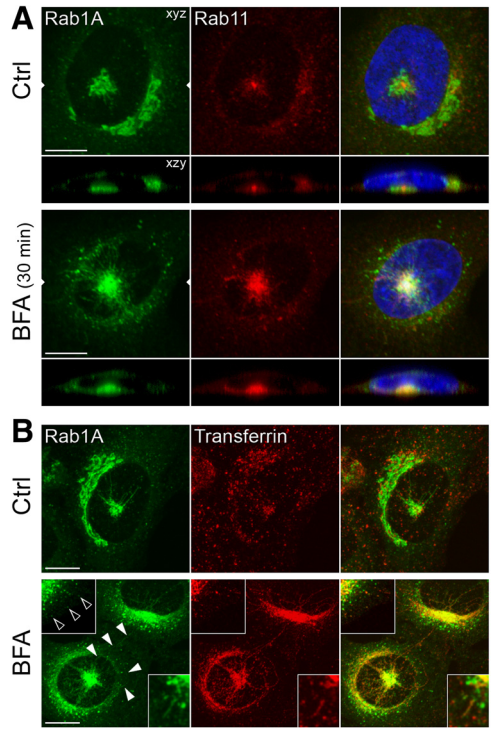

Figure 8. The pcIC and ERC constitute a stable pericentrosomal membrane system. A. NRK cells expressing GFP-Rab1A were stained with antibodies against Rab11, an ERC marker. Note partial colocalization of Rab1A and Rab11 under the nucleus in control cells (top panels) and the increased overlap of the pcIC and the expanded ERC in cells treated for 30 min with BFA (bottom panels). (B) Comparison of the localizations of GFP-Rab1A and transferrin. Note the distinct distributions of the two proteins in control cells (top panels), except for some overlap in the pericentrosomal area and peripheral IC elements (insets). By contrast, the two markers show extensive colocalization in BFA-treated cells, including the pcIC, the tubular IC network, and peripheral IC elements (top insets). Bars, 10 μm.

The IC Maintains Its Dynamic Properties in BFA-treated Cells

Because previous studies (Sannerud *et al.*, 2006) and the above data suggested that the IC maintains its dynamics in BFA-treated cells, we used spinning disk CM to follow GFP-Rab1A dynamics at various times (30–90 min) after drug addition. Indeed, the peripheral IC elements residing close to ERES (Figure 7B) continue to communicate with the pcIC via narrow tubules that either create transient connections, or bud off, move toward the pcIC, and merge with it. These events, together with the recruitment of GFP-Rab1A at the exit sites, can explain the oscillation of their fluorescent signals (Figure 7, A and C; Supplementary Movie 10), similar to that seen in control cells (Sannerud *et al.*, 2006). In addition, dynamic tubules continue to connect peripheral IC structures and also move to the cortical regions of the cell, giving rise to a widespread IC network (Figure 7, D and E; Supplementary Movies 11 and 12). The dynamic features of the IC remained unchanged at ~90 min after BFA addition, the last time point recorded (data not shown).

A Pericentrosomal Membrane System Consisting of pcIC and ERC

We next studied the relation to the pcIC with the Rab11-containing ERC, which in many cell types converges around the centrosome (Maxfield and McGraw, 2004). In control cells expressing a separate, GFP-Rab1A–positive pcIC below the nucleus, the ERC is found at the same

location, typically showing tight clustering around the centrosome (Figure 8A). After BFA treatment these compartments not only maintain their spatial connection, but increase their overlap due to preferential expansion of the ERC (Figure 8A). Although the ERC maintains its relatively compact appearance, the pcIC extends tubules toward the cell periphery (see Figure 7). The absence of Rab11 from these tubules suggested that the compartments remain as separate entities.

To reveal a possible functional link between the IC and the endosomal system, we first used transferrin (Tf), a commonly used reporter of endocytic recycling. After its uptake into sorting endosomes, Tf is partly transported to the ERC from which it returns to the PM still bound to its receptor (Maxfield and McGraw, 2004). Accordingly, after 60-min internalization, fluorescent Tf was found both in peripheral endosomes and the ERC of the GFP-Rab1A–expressing cells (Figure 8B). Although only a minor overlap was seen in control cells, BFA treatment resulted in redistribution of Tf to the Rab1A-positive pcIC and the associated tubular system (Figure 8B). Thus, in contrast to earlier studies concluding that Tf uses the tubular endosomal network during its recycling in BFA-treated NRK and HeLa cells (Lippincott-Schwartz *et al.*, 1991; Tooze and Hollingshead, 1992), the present results implicate the IC in this process. We propose that by affecting clathrin-mediated recycling of Tf from endosomes to the PM (Stoorvogel *et al.*, 1996; van Dam and Stoorvogel, 2002), BFA causes its accumulation in the ERC and subsequent transfer via the pcIC to the tubular IC network. Because the kinetics of recycling is not affected either by BFA (Lippincott-Schwartz *et al.*, 1991) or other inhibitors of clathrin function (Bennett *et al.*, 2001), Tf evidently can utilize the BFA-resistant, Rab1A-mediated pathway (Sannerud *et al.*, 2006) for its retrieval to the PM. A prerequisite for this unexpected journey is that Tf remains bound to its receptor (i.e., that the IC maintains an acidic lumenal pH; Palokangas *et al.*, 1998; Appenzeller-Herzog *et al.*, 2004).

The pcIC Operates As a Way Station in CFTR Trafficking

Finally, we addressed the role of the pcIC in biosynthetic trafficking of the CFTR, a chloride channel, which utilizes an unconventional, apparently Golgi-independent, but still poorly understood pathway to reach the PM (Bannykh *et al.*, 2000; Yoo *et al.*, 2002). Because the passage of viral proteins through the pcIC is inhibited at low temperatures (Figure 5), we examined if incubation at 15, 20, or 25°C has a similar effect on CFTR transport in stably transfected BHK cells. Although shift of cells to 15°C did not seem to affect CFTR localization, compared with 37°C (Figure 9, A and C), incubation at 20 or 25°C, correlating with increased rates of protein synthesis, resulted in its accumulation in a central, Rab1-positive compartment (Figure 9, B and C). Although mostly juxtanuclear (Figure 9B), these structures were also found below the nucleus (Figure 9, A and E), verifying that they correspond to the pcIC. To synchronize CFTR transport, we took advantage of the observation that long-term BFA treatment results in reversible arrest of the protein in the ER (Lukacs *et al.*, 1994; Okiyoneda *et al.*, 2004; Figure 9D). Localization of CFTR shortly after BFA washout in the presence of cycloheximide showed that it rapidly redistributes to the tubular IC network, including the centrally located pcIC (Figure 9E). Importantly, the transient accumulation of CFTR in the pcIC coincides with its rapid reexpression at the PM, but precedes the reassembly of the Golgi apparatus (Figure 9F). These results show that the pcIC functions as a way station during the trafficking of CFTR to the cell surface, a process that has been suggested to involve the endosomal system (Yoo *et al.*, 2002).

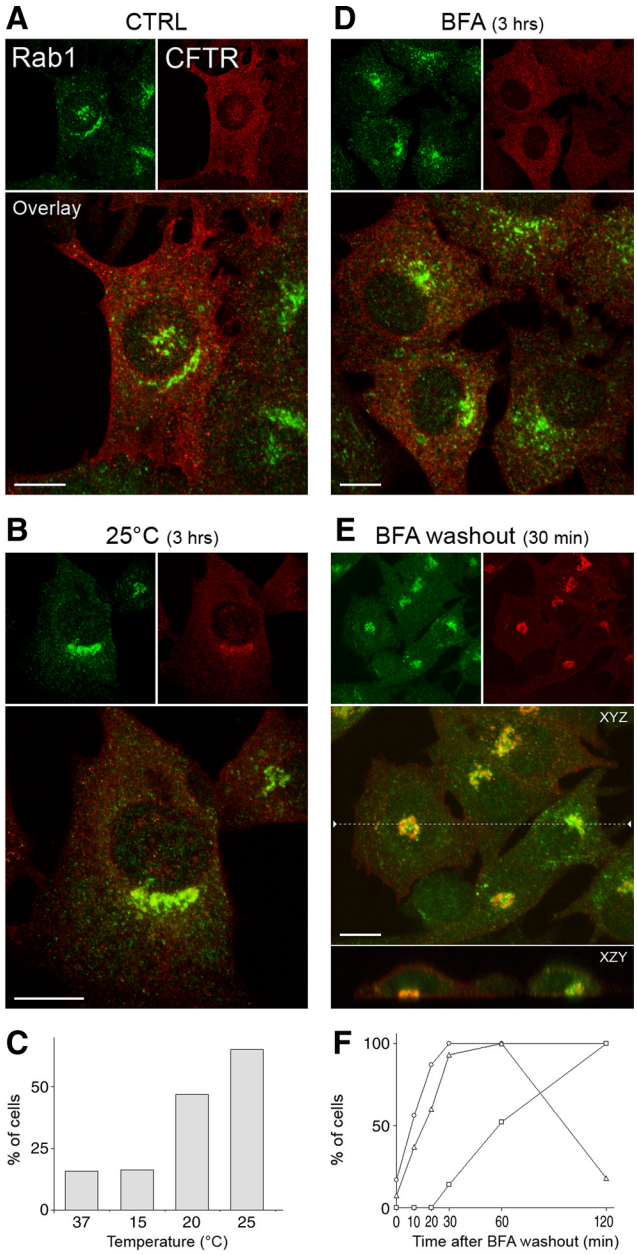

Figure 9. The pcIC acts in CFTR trafficking. (A–C) Localization of HA-tagged CFTR and endogenous Rab1 in BHK cells kept at 37°C or shifted for 3 h to 15, 20, or 25°C. A. Note the weak colocalization of the proteins in a control (37°C) cell expressing a separate pcIC and the lack of concentration of CFTR in the Golgi area. (B) After 25°C incubation the proteins show considerable overlap in a juxtanuclear structure. (C) Percentage of cells showing colocalization of CFTR and Rab1 at the different temperatures. (D and E) Localization of CFTR and Rab1 after 3 h BFA treatment (D) and 30 min after drug removal in the presence of cycloheximide (E). Note the ER-like pattern of CFTR after the BFA-treatment and its transfer to the Rab1-positive pcIC below the nucleus after BFA wash-out. The location of the XZY projection is shown by the dashed line in the XYZ image. (F) The percentage of cells showing colocalization of Rab1 and CFTR (△), expression of CFTR at the cell surface (○), or compact, juxtanuclear, mannosidase II-positive Golgis (□) was determined at different times after BFA washout.

DISCUSSION

Here we describe a novel subdomain of the IC (pcIC) by demonstrating the connection between Rab1A- and p58-positive IC elements and the centrosome. Crucial for the identification of the pcIC was the visualization of GFP-Rab1A dynamics in living cells, revealing its striking separation from the Golgi ribbon. The pcIC is a long-lived compartment equipped with transport machineries that communicates with peripheral IC elements and the Golgi stacks via two-way traffic. Thus, it can contain variable amounts of Golgi enzymes although it does not display Golgi-like, stacked morphology. Moreover, unlike the Golgi, the pcIC is resistant to BFA, persisting as the midpoint of a tubular network that connects with the cell periphery and participates in the drug-induced transfer of Golgi components to the ER. It also acts as a way station during Golgi relocation in motile cells, suggesting a role in Golgi biogenesis. Previously, based on its expansion, proposed biosynthetic functions (Sannerud *et al.*, 2006), and functional similarity with the ERC, we introduced the term biosynthetic recycling compartment (BRC) to describe the tubular domain of the IC defined by Rab1A (Saraste and Goud, 2007). The present results showing the stable connection of the pcIC and the ERC at the cell center seem to further justify the use of this term.

The separation of the pcIC from the Golgi is coupled to cell division and motility (i.e., events that involve Golgi disassembly or relocation), but it may also have other roles in cell physiology. Of practical importance, this rearrangement of the secretory apparatus allows more precise localization of various cargo, transport machinery, and signaling proteins at the IC–Golgi boundary. Based on the finding that ER-derived cargo is arrested in the pericentrosomal region at 20°C, it will also be of interest to study the relation of the pcIC/ERC system with the TGN, for example, by investigating the localization of proteins that have been assigned as components of the latter. For example, the finding of a distinct pool of COPI coats in the pcIC that is typically located next to the Golgi ribbon—and thus is obscured by it—could explain their reported association with the TGN (Griffiths *et al.*, 1995; Martinez-Menarguez *et al.*, 1999).

Imaging of GFP-Rab1A dynamics in BFA-treated cells showed that the pcIC is a major target not only for COPI-containing (Stephens and Pepperkok, 2002; Lippincott-Schwartz and Liu, 2006), but also COPI-free transport carriers originating close to the ERES (Figure 10). The latter may correspond to the ER-derived carriers that operate in the transport of GDI-anchored proteins in yeast and depend on functional Ypt1 (Rab1) for their formation (Morsomme and Riezman, 2002). The pcIC also extends tubules that frequently establish transient continuities with the *cis*-Golgi or peripheral ERES. Some of the tubules contain the KDEL-R, suggesting that they recycle proteins back to the ER (Simpson *et al.*, 2006). The function of the pcIC as a crossroads station in secretory trafficking (Figure 10) can also explain the effect of low temperature on the passage of cargo through this compartment (Kuismanen and Saraste, 1989). Moreover, the binding of COPI coats to the pcIC underscores its function in molecular sorting.

Based on the present results, the IC could be seen as an autonomous organelle whose sorting and transport activities create the functional boundary between the ER and the Golgi apparatus. The segregation of forward-directed molecules from recycled components within the IC network could be achieved via multiple sorting and transport steps (Figure 10) involving different COPI coats, Rab proteins, fusion factors (tethers and SNAREs), and molecular motors. The coiled coil proteins GMAP-210 and Hook3, which have been proposed to attach *cis*-Golgi membranes to the minus ends of MTs (Walenta *et al.*, 2001; Rios *et al.*, 2004), are candidates to anchor the pcIC to the pericentrosomal region. Notably, the latter maintains its juxtanuclear localization after BFA treatment (Walenta *et al.*, 2001). The pcIC–centrosome connection further implies that transport from peripheral ERES via the pcIC to the *cis*-Golgi requires both dynein and kinesin motors (Figure 10), which associate with the IC membranes (Lippincott-Schwartz *et al.*, 2000; Allan *et al.*, 2002).

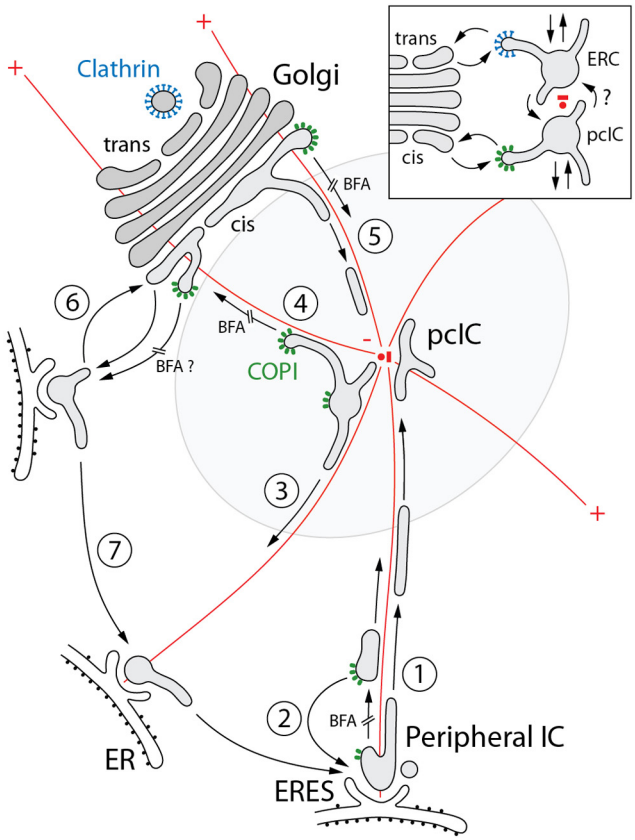

Figure 10. Pathways of membrane traffic at the ER–Golgi boundary. Based on the identification of the pcIC, localization of marker proteins, and imaging of IC dynamics in control and BFA-treated cells, a working model is presented for forward transport and membrane recycling at the ER–Golgi boundary. The different transport steps are numbered and the BFA-sensitive steps are indicated. The centrosome with its radiating MTs (red) and the distinct pools of COPI coats (green) are shown in color. Steps 1 and 2: Forward transport from peripheral IC to the pcIC involves MT-based centralization of COP-dependent and -independent carriers. Step 3: Membrane recycling from the pcIC to peripheral IC/ERES can also occur in a COPI-independent manner. Forward transport (step 4) and membrane recycling (step 5) at the pcIC-Golgi boundary involve COPI-dependent and -independent pathways, respectively. Step 6: Two-way ER–Golgi traffic may also take place between Golgi stacks and nearby ERES. In addition to steps 5 and 3, this transport step (step 6) and dynamic, possibly actin-mediated, connections between peripheral IC elements (step 7) could contribute to BFA-induced redistribution of Golgi components to the ER and also explain their MT-independent redistribution to peripheral IC/ERES. The inset shows a model proposing bidirectional communication between the pcIC and the ERC. Putative clathrin coats operating in transport between the ERC and *trans*-Golgi are shown in blue color. See the text for further discussion.

Reinforcing early ideas on a dual role of COPI in forward transport and recycling (Bannykh *et al.*, 1998; Lowe and Kreis, 1998), we propose that transport from pcIC to *cis*-Golgi depends on these coats (Figure 10), possibly coinciding with a key step in Golgi biogenesis that is regulated by Rab1 (Haas *et al.*, 2007). Although many proteins require COPI function for ER exit (Altan-Bonnet *et al.*, 2004), inhibition of this novel anterograde transport step may be a major reason for Golgi disassembly in BFA-treated cells, leading to COPI-independent transfer of its components to the pcIC (Figure 10). However, the BFA-induced backflow of Golgi proteins to the ER may not exclusively occur via the pcIC, but also involves ERES located close to the Golgi stacks (Figure 10). Direct communication between the Golgi and such nearby ERES, occurring in a MT-independent manner or involving Golgi-nucleated, more stable MTs, could explain the redistribution of the Golgi during the depolymerization of MTs, as well as contribute to the maintenance of the integrity of this organelle as it becomes separated from the centrosome and the pcIC/ERC.

The existence of at least three biochemically distinct COPI coats in mammalian cells (Wegmann *et al.*, 2004) correlates with COPI association with peripheral IC, pcIC, and *cis*-Golgi (Golgi stack) membranes (Figure 10). The operation of COPI isotypes and COPI-independent pathways allows molecules to employ alternative routes, as exemplified by the differential localization of p58 and the KDEL-R in BFA-treated cells. Evidently, p58 can recycle from the pcIC and *cis*-Golgi after coat disassembly, accumulating in the peripheral IC at ERES, because its forward transport requires COPI function (Saraste and Svensson, 1991; Ward *et al.*, 2001). By contrast, the KDEL-R maintains its colocalization with Rab1 in the drug-treated cells, apparently because of its ability to cycle between the peripheral IC and pcIC in a COPI-independent manner. The COPI vesicles found in the Golgi area, containing the KDEL-R or p58/ERGIC-53 (Griffiths *et al.*, 1994; Orci *et al.*, 1997; Klumperman *et al.*, 1998; Martinez-Menarguez *et al.*, 1999), could also operate in the transfer of these proteins from the pcIC to the *cis*-Golgi.

Finally, our results reveal a novel spatial organization of the secretory pathway by placing the Rab1A-containing pcIC next to the Rab11-positive ERC that typically converges around the centrosome. This pericentrosomal membrane system evidently communicates with the *cis* and *trans* sides of the Golgi stacks (Figure 10, inset; Bonifacino and Rojas, 2006; present results) and, based on GFP-Rab1A dynamics and the localization of Golgi proteins, this communication is not prevented, but may be modulated, when these compartments move away from the Golgi ribbon. The BFA-resistant juxtaposition of the pcIC and ERC raises the possibility that they establish stable membrane contact sites that facilitate the exchange of ions, lipids or sterols (Levine, 2004). Moreover, our results on CFTR trafficking and transferrin recycling indicate that these compartments are connected via membrane traffic.

Regarding biosynthetic trafficking, studies of the yeast *Saccharomyces cerevisiae* have revealed functional links between Ypt1 and Ypt31/32, the yeast counterparts of mammalian Rab1 and Rab11 (Yang *et al.*, 1998; Sacher *et al.*, 2008). For example, two conserved tethers (TRAPPI and TRAPPII) have been implicated as GEFs during the activation of Ypt1 (Rab1) and Ypt31/32 (Sacher *et al.*, 2008; Yamasaki *et al.*, 2009). Interestingly, mammalian Bet3p, one of the common subunits of these complexes that acts in ER–Golgi trafficking, localizes in NRK cells to a BFA-resistant juxtanuclear structure (Yu *et al.*, 2006), which most likely corresponds to the pcIC described here. Direct connection(s) between the IC and the endosomal system (Figure 10, inset) could explain the transport of cholesterol and certain types of membrane proteins to the PM even in the presence of BFA (Urbani and Simoni, 1990; Marie *et al.*, 2008), because the dynamics of the IC (Sannerud *et al.*, 2006; present results) and the endocytic apparatus (Klausner *et al.*, 1992; Bonifacino and Rojas, 2006) remain largely unaffected by this drug. Future studies using live cell imaging, electron microscopy and biochemical methods should provide further insight into the structure and function of this novel pericentrosomal membrane system in different cell types and physiological conditions, as well as its role during cell division.

ACKNOWLEDGMENTS

This article is dedicated to the memory of George Palade (1912–2008). We are grateful to Michel Bornens, Michael Caplan, Bruno Goud, Jussi Jäntti, Esa Kuismanen, Kristian Prydz, Kirsten Sandvig, Anni Vedeler, and Theresa Ward for helpful discussions and George Banting, Michel Bornens, Bruno Goud, Wanjin Hong, Margaret Kielian, Esa Kuismanen, Irina Majoul, and Kelley Moremen for generously providing antibodies. The BHK cells stably expressing CFTR were a kind gift from Gergely Lukacs (McGill University). This work was supported by the Medical Faculty of the University of Bergen, The Norwegian Cancer Society, Helse-Vest, and The Functional Genomics (FUGE) Program of the Research Council of Norway.

REFERENCES

Allan, B. B., Moyer, B. D., and Balch, W. E. (2000). Rab1 recruitment of p115 into a *cis*-SNARE complex: programming budding COPII vesicles for fusion. Science *289*, 444–448.

Allan, V. J., Thompson, H., and McNiven, M. A. (2002). Motoring around the Golgi. Nat. Cell Biol. *4*, 236–242.

Altan-Bonnet, N., Sougrat, R., and Lippincott-Schwartz, J. (2004). Molecular basis for Golgi maintenance and biogenesis. Curr. Opin. Cell Biol. *16*, 364–372.

Ang, A. L., Taguchi, T., Francis, S., Folsch, H., Murrells, L. J., Pypaert, M., Warren, G., and Mellman, I. (2004). Recycling endosomes can serve as intermediates during transport from the Golgi to the plasma membrane of MDCK cells. J. Cell Biol. *167*, 531–543.

Appenzeller-Herzog, C., Roche, A. C., Nufer, O., and Hauri, H.-P. (2004). pH-induced conversion of the transport lectin ERGIC-53 triggers glycoprotein release. J. Biol. Chem. *279*, 12943–12950.

Bannykh, S. I., Rowe, T., and Balch, W. E. (1996). The organization of endoplasmic reticulum export complexes. J. Cell Biol. *135*, 19–35.

Bannykh, S. I., Nishimura, N., and Balch, W. E. (1998). Getting into the Golgi. Trends Cell Biol. *8*, 21–25.

Bannykh, S. I., Bannykh, G. I., Fish, K. N., Moyer, B. D., Riordan, J. R., and Balch, W. E. (2000). Traffic pattern of cystic fibrosis transmembrane regulator through the early exocytic pathway. Traffic *1*, 852–870.

Barzilay, E., Ben-Califa, N., Hirschberg, K., and Neumann, D. (2005). Uncoupling of brefeldin A-mediated coatomer protein complex-I dissociation from Golgi redistribution. Traffic *6*, 794–802.

Bennett, E. M., Lin, S. X., Towler, M. C., Maxfield, F. R., and Brodsky, F. M. (2001). Clathrin hub expression affects early endosome distribution with minimal impact on receptor sorting and recycling. Mol. Biol. Cell *12*, 2790–2799.

Bisel, B., Wang, Y., Wei, J. H., Xiang, Y., Tang, D., Miron-Mendoza, M., Yoshimura, S., Nakamura, N., and Seemann, J. (2008). ERK regulates Golgi and centrosome orientation towards the leading edge through GRASP65. J. Cell Biol. *182*, 837–843.

Bonifacino, J. S., and Rojas, R. (2006). Retrograde transport from endosomes to the *trans*-Golgi network. Nat. Rev. Mol. Cell Biol. *7*, 568–579.

Chabin-Brion, K., Marceiller, J., Perez, F., Settegrana, C., Drechou, A., Durand, G., and Poüs, C. (2001). The Golgi complex is a microtubule-organizing organelle. Mol. Biol. Cell *12*, 2047–2060.

De Matteis, M. A., and Luini, A. (2008). Exiting the Golgi complex. Nat. Rev. Mol. Cell Biol. *9*, 273–284.

Egea, G., Lázaro-Diéguez, F., and Vilella, M. (2006). Actin dynamics at the Golgi complex in mammalian cells. Curr. Opin. Cell Biol. *18*, 168–178.

Futter, C. E., Connolly, C. N., Cutler, D. F., and Hopkins, C. R. (1995). Newly synthesized transferrin receptors can be detected in the endosome before they appear on the cell surface. J. Biol. Chem. *270*, 10999–11003.

Gaynor, E. C., and Emr, S. D. (1997). COPI-independent anterograde transport: cargo-selective ER to Golgi protein transport in yeast COPI mutants. J. Cell Biol. *136*, 789–802.

Girod, A., Storrie, B., Simpson, J. C., Johannes, L., Goud, B., Roberts, L. M., Lord, J. M., Nilsson, T., and Pepperkok, R. (1999). Evidence for a COPI-independent transport route from the Golgi complex to the endoplasmic reticulum. Nat. Cell Biol. *1*, 423–430.

Glick, B. S., Elston, T., and Oster, G. (1997). A cisternal maturation mechanism can explain the asymmetry of the Golgi stack. FEBS Lett. *414*, 177–181.

Gravotta, D., Deora, A., Perret, E., Oyanadel, C., Soza, A., Schreiner, R., Gonzalez, A., and Rodriguez-Boulan, E. (2007). AP1B sorts basolateral proteins in recycling and biosynthetic routes of MDCK cells. Proc. Natl. Acad. Sci. USA *104*, 1564–1569.

Griffiths, G., and Simons, K. (1986). The *trans*-Golgi network: sorting at the exit site of the Golgi complex. Science *234*, 438–443.

Griffiths, G., Ericsson, M., Krijnse-Locker, J., Nilsson, T., Goud, B., Söling, H. D., Tang, B. L., Wong, S. H., and Hong, W. (1994). Localization of the Lys, Asp, Glu, Leu tetrapeptide receptor to the Golgi complex and the intermediate compartment in mammalian cells. J. Cell Biol. *127*, 1557–1574.

Griffiths, G., Pepperkok, R., Krijnse-Locker, J., and Kreis, T. E. (1995)., Immunocytochemical localization of β-COP to the ER-Golgi boundary and the TGN. J. Cell Sci. *108*, 2839–2856.

Haas, A. K., Yoshimura, S., Stephens, D. J., Preisinger, C., Fuchs, E., and Barr, F. A. (2007). Analysis of GTPase-activating proteins: Rab1 and Rab43 are key Rabs required to maintain a functional Golgi complex in human cells. J. Cell Sci. *120*, 2997–3010.

Hammond, A. T., and Glick, B. S. (2000). Dynamics of transitional endoplasmic reticulum sites in vertebrate cells. Mol. Biol. Cell *11*, 3013–3030.

Harsay, E., and Schekman, R. (2002). A subset of yeast vacuolar protein sorting mutants is blocked in one branch of the exocytic pathway. J. Cell Biol. *156*, 271–285.

Hawes, C., Osterrieder, A., Hummel, E., and Sparkes, I. (2008). The plant ER-Golgi interface. Traffic *9*, 1571–1580.

Hedman, K., Goldenthal, K. L., Rutherford, A. V., Pastan, I., and Willingham, M. C. (1987). Comparison of the intracellular pathways of transferrin recycling and vesicular stomatitis virus membrane glycoprotein exocytosis by ultrastructural double-label cytochemistry. J. Histochem. Cytochem. *35*, 233–243.

Heino, S., Lusa, S., Somerharju, P., Ehnholm, C., Olkkonen, V. M., and Ikonen, E. (2000). Dissecting the role of the Golgi complex and lipid rafts in biosynthetic transport of cholesterol to the cell surface. Proc. Natl. Acad. Sci. USA *97*, 8375–8380.

Horstmann, H., Ng, C. P., Tang, B. L., and Hong, W. (2002). Ultrastructural characterization of endoplasmic reticulum-Golgi transport containers (EGTCs). J. Cell Sci. *115*, 4263–4273.

Kappeler, F., Klopfenstein, D. R., Foguet, M., Paccaud, J. P., and Hauri, H. P. (1997). The recycling of ERGIC-53 in the early secretory pathway. ERGIC-53 carries a cytosolic endoplasmic reticulum-exit determinant interacting with COPII. J. Biol. Chem. *272*, 31801–31808.

Karolewski, B. A., Watson, D. J., Parente, M. K., and Wolfe, J. H. (2003). Comparison of transfection conditions for a lentivirus vector produced in large volumes. Hum. Gene Ther. *14*, 1287–1296.

Klausner, R. D., Donaldson, J. G., and Lippincott-Schwartz, J. (1992). Brefeldin A: insights into the control of membrane traffic and organelle structure. J. Cell Biol. *116*, 1071–1080.

Klumperman, J., Schweizer, A., Clausen, H., Tang, B. L., Hong, W., Oorschot, V., and Hauri, H. P. (1998). The recycling pathway of protein ERGIC-53 and dynamics of the ER-Golgi intermediate compartment. J. Cell Sci. *111*, 3411–3425.

Kodani, A., and Sütterlin, C. (2008). The Golgi protein GM130 regulates centrosome morphology and function. Mol. Biol. Cell *19*, 745–753.

Kuismanen, E., and Saraste, J. (1989). Low temperature-induced transport blocks as tools to manipulate membrane traffic. Methods Cell Biol. *32*, 257–274.

Ladinsky, M. S., and Howell, K. E. (1992). The *trans*-Golgi network can be dissected structurally and functionally from the cisternae of the Golgi complex by brefeldin A. Eur. J. Cell Biol. *59*, 92–105.

Leitinger, B., Hille-Rehfeld, A., and Spiess, M. (1995). Biosynthetic transport of the asialoglycoprotein receptor H1 to the cell surface occurs via endosomes. Proc. Natl. Acad. Sci. USA *92*, 10109–10113.

Levine, T. (2004). Short-range intracellular trafficking of small molecules across endoplasmic reticulum junctions. Trends Cell Biol. *14*, 483–490.

Lippincott-Schwartz, J., Yuan, L., Tipper, C., Amherdt, M., Orci, L., and Klausner, R. D. (1991). Brefeldin A's effects on endosomes, lysosomes, and the TGN suggest a general mechanism for regulating organelle structure and membrane traffic. Cell *67*, 601–616.

Lippincott-Schwartz, J., Roberts, T. H., and Hirschberg, K. (2000). Secretory protein trafficking and organelle dynamics in living cells. Annu. Rev. Cell Dev. Biol. *16*, 557–589.

Lippincott-Schwartz, J., and Liu, W. (2006). Insights into COPI coat assembly and function in living cells. Trends Cell Biol. *16*, 1–4.

Lock, J. G., and Stow, J. L. (2005). Rab11 in recycling endosomes regulates the sorting and basolateral transport of E-cadherin. Mol. Biol. Cell *16*, 1744–1755.

Lowe, M., and Kreis, T. E. (1998). Regulation of membrane traffic in animal cells by COPI. Biochim. Biophys. Acta *1404*, 53–66.

Lukacs, G. L., Mohamed, A., Kartner, N., Chang, X. B., Riordan, J. R., and Grinstein, S. (1994). Conformational maturation of CFTR but not its mutant counterpart (rF508) occurs in the endoplasmic reticulum and requires ATP. EMBO J. *13*, 6076–6086.

Malsam, J., Satoh, A., Pelletier, L., and Warren, G. (2005). Golgin tethers define subpopulations of COPI vesicles. Science *307*, 1095–1098.

Manolea, F., Claude, A., Chun, J., Rosas, J., and Melancon, P. (2008). Distinct functions for Arf nucleotide exchange factors at the Golgi complex: GBF1 and BIGs are required for assembly and maintenance of the Golgi stack and TGN, respectively. Mol. Biol. Cell *19*, 523–535.

Marie, M., Sannerud, R., Dale, H. A., and Saraste, J. (2008). Take the 'A' train: on fast tracks to the cell surface. Cell Mol. Life Sci. *65*, 2859–2874.

Martinez-Menarguez, J. A., Geuze, H. J., Slot, J. W., and Klumperman, J. (1999). Vesicular tubular clusters between the ER and Golgi mediate concentration of soluble secretory proteins by exclusion from COPI-coated vesicles. Cell *98*, 81–90.

Maxfield, F. R., and McGraw, T. E. (2004). Endocytic recycling. Nat. Rev. Mol. Cell Biol. *5*, 121–132.

Moelleken, J., *et al.* (2007). Differential localization of coatomer complex isoforms within the Golgi apparatus. Proc. Natl. Acad. Sci. USA *104*, 4425–4430.

Monetta, P., Slavin, I., Romero, N., and Alvarez, C. (2007). Rab1B interacts with GBF1 and modulates both ARF1 dynamics and COPI association. Mol. Biol. Cell *18*, 2400–2410.

Moremen, K. W., and Touster, O. (1985). Biosynthesis and modification of Golgi mannosidase II in HeLa and 3T3 cells. J. Biol. Chem. *260*, 6654–6662.

Morsomme, P., and Riezman, H. (2002). The Rab GTPase Ypt1p and tethering factors couple protein sorting at the ER to vesicle targeting to the Golgi apparatus. Dev. Cell *2*, 307–317.

Okiyoneda, T., Harada, K., Yamahira, K., Wada, I., Hashimoto, Y., Ueno, K., Suico, M. A, Shuto, T., and Kai, H. (2004). Characterization of the trafficking pathway of cystic fibrosis transmembrane conductance regulator in baby hamster kidney cells. J. Pharmacol. Sci. *95*, 471–475.

Orci, L., Stamnes, M., Ravazzola, M., Amherdt, M., Perrelet, A., Söllner, T. H., and Rothman, J. E. (1997). Bidirectional transport by distinct populations of COPI-coated vesicles. Cell *90*, 335–349.

Orzech, E., Cohen, S., Weiss, A., and Aroeti, B. (2000). Interactions between the exocytic and endocytic pathways in polarized Madin-Darby canine kidney cells. J. Biol. Chem. *275*, 15207–15219.

Palade, G. E. (1982). Problems in intracellular membrane traffic. In: Ciba Foundation Symposium *92*, Membrane Recycling, ed. D. Evered and G. M. Collins, London: Pitman Books, 1–14.

Palokangas, H., Ying, M., Väänänen, K., and Saraste, J. (1998). Retrograde transport from the pre-Golgi intermediate compartment and the Golgi complex is affected by the vacuolar H^+-ATPase inhibitor bafilomycin A1. Mol. Biol. Cell *9*, 3561–3578.

Paroutis, P., Touret, N., and Grinstein, S. (2004). The pH of the secretory pathway: measurement, determinants, and regulation. Physiology *19*, 207–215.

Pepperkok, R., Scheel, J., Horstmann, H., Hauri, H.-P., Griffiths, G., and Kreis, T. E. (1993). β-COP is essential for biosynthetic membrane transport from the endoplasmic reticulum to the Golgi complex in vivo. Cell *74*, 71–82.

Peter, F., Plutner, H., Zhu, H., Kreis, T. E., and Balch, W. E. (1993). β-COP is essential for transport of protein from the endoplasmic reticulum to the Golgi in vitro. J. Cell Biol. *122*, 1155–1167.

Presley, J. F., Cole, N. B., Schroer, T. A., Hirschberg, K., Zaal, K. J., and Lippincott-Schwartz, J. (1997). ER-to-Golgi transport visualized in living cells. Nature *389*, 81–85.

Reaves, B., and Banting, G. (1992). Perturbation of morphology of the *trans*-Golgi network following brefeldin A treatment: redistribution of a TGN-specific integral membrane protein, TGN38. J. Cell Biol. *116*, 85–94.

Rios, R. M., and Bornens, M. (2003). The Golgi apparatus at the cell centre. Curr. Opin. Cell Biol. *15*, 60–66.

Rios, R. M., Sanchis, A., Tassin, A. M., Fedriani, C., and Bornens, M. (2004). GMAP-210 recruits γ-tubulin complexes to *cis*-Golgi membranes and is required for Golgi ribbon formation Cell *118*, 323–335.

Sacher, M., Kim, Y. G., Lavie, A., Oh, B. H., and Segev, N. (2008). The TRAPP complex: insights into its architecture and function. Traffic *9*, 2032–2042.

Sallese, M., Pulvirenti, T., and Luini, A. (2006). The physiology of membrane transport and endomembrane-based signalling. EMBO J. *25*, 2663–2673.

Sandvig, K., and van Deurs, B. (2002). Transport of protein toxins into cells: pathways used by ricin, cholera toxin and shiga toxin. FEBS Lett. *529*, 49–53.

Sannerud, R., Marie, M., Nizak, C., Dale, H. A., Pernet-Gallay, K., Perez, F., Goud, B., and Saraste, J. (2006). Rab1 defines a novel pathway connecting the pre-Golgi intermediate compartment with the cell periphery. Mol. Biol. Cell *17*, 1514–1526.

Sannerud, R., Marie, M., Hansen, B. B., and Saraste, J. (2008). Use of polarized PC12 cells to monitor protein localization in the early biosynthetic pathway. Meth. Mol Biol. *457*, 253–265.

Saraste, J., and Kuismanen, E. (1984). Pre- and post-Golgi vacuoles operate in the transport of Semliki Forest virus membrane glycoproteins to the cell surface. Cell *38*, 535–549.

Saraste, J., and Svensson, K. (1991). Distribution of the intermediate elements operating in ER to Golgi transport. J. Cell Sci. *100*, 415–430.

Saraste, J., and Kuismanen, E. (1992). Pathways of protein sorting and membrane traffic between the rough endoplasmic reticulum and the Golgi complex. Semin. Cell Biol. *3*, 343–355.

Saraste, J., Lahtinen, U., and Goud, B. (1995). Localization of the small GTP-binding protein Rab1 to early compartments of the secretory pathway. J. Cell Sci. *108*, 1541–1552.

Saraste, J., and Goud, B. (2007). Functional symmetry of endomembranes. Mol. Biol. Cell *18*, 1430–1436.

Scales, S. J., Pepperkok, R., and Kreis, T. E. (1997). Visualization of ER-to-Golgi transport in living cells reveals a sequential mode of action for COPII and COPI. Cell *90*, 1137–1148.

Sciaky, N., Presley, J., Smith, C., Zaal, K. J., Cole, N., Moreira, J. E., Terasaki, M., Siggia, E., and Lippincott-Schwartz, J. (1997). Golgi tubule traffic and the effects of brefeldin A visualized in living cells. J. Cell Biol. *139*, 1137–1155.

Sharma, M., *et al.* (2004). Misfolding diverts CFTR from recycling to degradation: quality control at early endosomes. J. Cell Biol. *164*, 923–933.

Simpson, J. C., Nilsson, T., and Pepperkok, R. (2006). Biogenesis of tubular ER-to-Golgi transport inter-mediates. Mol. Biol. Cell *17*, 723–737.

Stephens, D. J., and Pepperkok, R. (2002). Imaging of procollagen transport reveals COPI-dependent cargo sorting during ER-to-Golgi transport in mammalian cells. J. Cell Sci. *115*, 1149–1160.

Stoorvogel, W., Oorschot, V., and Geuze, H. J. (1996). A novel class of clathrin-coated vesicles budding from endosomes. J. Cell Biol. *132*, 21–33.

Sütterlin, C., Hsu, P., Mallabiabarrena, A., and Malhotra, V. (2002). Fragmentation and dispersal of the pericentriolar Golgi complex is required for entry into mitosis in mammalian cells. Cell *109*, 359–369.

Sztul, E., and Lupashin, V. (2006). Role of tethering factors in secretory membrane traffic. Am. J. Physiol. Cell Physiol. *290*, C11–C26.

Thyberg, J., and Moskalewski, S. (1999). Role of microtubules in the organization of the Golgi complex. Exp. Cell Res. *246*, 263–279.

Tisdale, E. J., Plutner, H., Matteson, J., and Balch, W. E. (1997). p53/58 binds COPI and is required for selective transport through the early secretory pathway. J. Cell Biol. *137*, 581–593.

Tooze, J., and Hollinshead, M. (1992). In AtT20 and HeLa cells brefeldin A induces the fusion of tubular endosomes and changes their distribution and some of their endocytic properties. J. Cell Biol. *118*, 813–830.

Trucco, A., *et al.* (2004). Secretory traffic triggers the formation of tubular continuities across Golgi sub-compartments. Nat. Cell Biol. *6*, 1071–1081.

Urbani, L., and Simoni, R. D. (1990). Cholesterol and vesicular stomatitis virus G protein take separate routes from the endoplasmic reticulum to the plasma membrane. J. Biol. Chem. *265*, 1919–1923.

van Dam, E. M., and Stoorvogel, W. (2002). Dynamin-dependent transferrin receptor recycling by endosome-derived clathrin-coated vesicles. Mol. Biol. Cell *13*, 169–182.

Walenta, J. H., Didier, A. J., Liu, X., and Krämer, H. (2001). The Golgi-associated Hook3 protein is a member of a novel family of microtubule-binding proteins. J. Cell Biol. *152*, 923–934.

Ward, T. H., Polishchuk, R. S., Caplan, S., Hirschberg, K., and Lippincott-Schwartz, J. (2001). Maintenance of Golgi structure and function depends on the integrity of ER export. J. Cell Biol. *155*, 557–570.

Wegmann, D., Hess, P., Baier, C., Wieland, F. T., and Reinhard, C. (2004). Novel isotypic γ/ζ subunits reveal three coatomer complexes in mammals. Mol. Cell. Biol. *24*, 1070–1080.

Wood, S. A., Park, J. E., and Brown, W. J. (1991). Brefeldin A causes a microtubule-mediated fusion of the trans-Golgi network and early endosomes. Cell *67*, 591–600.

Yamasaki, A., Menon, S., Yu, S., Barrowman, J., Meerloo, T., Oorschot, V., Klumperman, J., Satoh, A., and Ferro-Novick, S. (2009). mTrs130 is a component of a mammalian TRAPPII complex, a Rab1 GEF that binds to COPI coated vesicles. Mol. Biol. Cell *20*, 4205–4215.

Yang, X., Matern, H. T., and Gallwitz, D. (1998). Specific binding to a novel and essential Golgi membrane protein (Yip1p) functionally links the transport GTPases Ypt1p and Ypt31p. EMBO J. *17*, 4954–4963.

Ying, M., Flatmark, T., and Saraste, J. (2000). The p58-positive pre-Golgi intermediates consist of distinct subpopulations of particles that show differential binding of COPI and COPII coats and contain vacuolar H^+-ATPase. J. Cell Sci. *113*, 3623–3638.

Yoo, J. S., Moyer, B. D., Bannykh, S., Yoo, H. M., Riordan, J. R., and Balch, W. E. (2002). Non-conventional trafficking of the cystic fibrosis transmembrane conductance regulator through the early secretory pathway. J. Biol. Chem. *277*, 11401–11409.

Yu, S., Satoh, A., Pypaert, M., Mullen, K., Hay, J. C., and Ferro-Novick, S. (2006). mBet3p is required for homotypic COPII vesicle tethering in mammalian cells. J. Cell Biol. *174*, 359–368.